



OPEN Seed metabolomic profiling of contrasting mung bean (*Vigna radiata*) genotypes under heat stress

Uday Chand Jha^{1,2}, Harsh Nayyar³, Shyam Tallury⁴, Kadambot H. M. Siddique⁵, Ignacio A. Ciampitti⁶ & P. V. Vara Prasad²

Mung bean (*Vigna radiata*), a high-value leguminous crop essential for global nutritional security, suffers substantial yield losses due to increasing heat stress. While numerous studies have explored the physiological and biochemical mechanisms underlying heat stress tolerance in mung bean, the effects of heat stress on grain quality at the metabolomic level remain largely unexplored. This study presents the first comprehensive analysis of heat stress-responsive seed metabolite changes in two contrasting mung bean genotypes—the heat-tolerant (HT) PI425243 and the heat-sensitive (HS) PI223002—using an untargeted metabolomics approach. Volcano plot analysis identified 68 significant metabolites (39 upregulated and 29 downregulated) under heat stress, based on a VIP value > 1.5; \log_2 fold-change ≥ 1 (upregulated) or ≤ -1 (downregulated), and $p < 0.05$. Notably, several metabolites, including hydrocinnamic acid, 5-hydroxyferulic acid, quercetin, myricetin, kaempferol 3-(2G-apiosylrobinobioside), and hesperetin 7-neohesperidoside, showed higher accumulation in PI425243 than in PI223002, potentially contributing to the maintenance of grain quality under heat stress. Metabolic pathway enrichment analysis further revealed the active involvement of starch and sucrose metabolism, tyrosine metabolism, steroid hormone biosynthesis, and caffeine metabolism in mediating heat stress response and tolerance. These metabolites could serve as potential biomarkers for identifying heat-tolerant mung bean genotypes and sustaining yield under high-temperature environments.

Keywords Mungbean, Metabolomics, Seed, Heat stress, Climate change

Mung bean (*Vigna radiata*) is a globally important pulse crop, valued for its high nutritional content and agronomic versatility. It is a rich source of easily digestible protein, essential macro- and micronutrients—including phosphorus, magnesium, potassium, zinc, iron, copper, manganese, and vitamins A, B₂, and B₆—along with dietary fiber and various bioactive compounds beneficial to human health^{1,2}. Consequently, mung bean serves as a vital cash crop for smallholder farmers and plays a crucial role in combating global hunger and malnutrition, particularly in South and Southeast Asia.

Globally, mung bean is cultivated on approximately 7 million hectares, with Asia (mainly India, Myanmar, China, Pakistan, and Thailand) accounting for about 90% of production, averaging 721 kg/ha³. India produces about 1.6 million tonnes (Mt), followed closely by Myanmar at 1.59 Mt⁴. As a legume, mung bean enhances soil fertility by fixing atmospheric nitrogen through root-associated rhizobacteria, thereby supporting sustainable agroecosystems⁵. Its short growth cycle also makes it suitable for intercropping and double-cropping systems⁶.

Mung bean productivity is increasingly limited by multiple abiotic stresses, notably drought, salinity, flooding, and heat stress. Under ongoing climate change, rising global temperatures pose a major threat to mung bean yield, as heat stress affects both vegetative and reproductive development^{7–9}. During the vegetative phase, high temperatures impair key physiological processes such as photosynthesis, respiration, transpiration, and

¹Indian Council for Agricultural Research (ICAR) - Indian Institute of Pulses Research (IIPR), Kanpur, Uttar Pradesh 208024, India. ²Department of Agronomy, Kansas State University, Manhattan, KS 66506, USA. ³Department of Botany, Panjab University, Chandigarh 160014, India. ⁴Plant Genetic Resources Conservation Unit in Griffin, Griffin, GA 30223, USA. ⁵The UWA Institute of Agriculture, The University of Western Australia, Crawley, Perth 6009, Australia. ⁶Department of Agronomy, Purdue University, West Lafayette, IN, USA. ✉email: u9811981@gmail.com; harshnayyar@hotmail.com; vara@ksu.in

stomatal conductance, while damaging the photosynthetic apparatus^{9,10}. More critically, heat stress during the reproductive phase drastically reduces productivity by inducing excessive flower drop and impairing pollen formation, viability, germination, and stigma receptivity, ultimately resulting in malformed pods and seeds and thus reduced yield^{2,9,10}.

Although substantial research has elucidated the physiological and biochemical mechanisms underlying heat tolerance, as well as its effects on seed quality traits such as protein and nutrient composition^{2,10}, the metabolomic basis of heat stress response in mung bean seeds remains largely uncharacterized. Metabolomics provides a powerful means of profiling the complete set of metabolites within a biological system at a given time, enabling insights into the metabolic adjustments underpinning stress adaptation^{11–13}. This approach has been pivotal in uncovering key heat-responsive metabolites and pathways in several crops, including rice (*Oryza sativa* L.)^{11,14,15}, maize (*Zea mays* L.)^{12,16–18}, wheat (*Triticum aestivum*)^{19–22}, sorghum (*Sorghum bicolor*)²³, *Medicago sativa*¹³, soybean (*Glycine max* L.)^{24,25} and chickpea (*Cicer arietinum* L.)^{26,27}.

Despite these advances, metabolomic studies aimed at deciphering the mechanisms of heat tolerance in mung bean are scarce. Therefore, this study employs an untargeted metabolomics approach to characterize the seed metabolite profiles of two contrasting mung bean genotypes—one heat-tolerant and one heat-sensitive—under controlled heat stress (42/30 °C) conditions, providing novel insights into the metabolic basis of heat stress tolerance in this important crop.

Material and methods

Plant material and growth conditions

Two contrasting mung bean genotypes—PI425243 (heat-tolerant; HT) and PI223002 (heat-sensitive; HS)²—were cultivated under controlled environment conditions in a greenhouse. Plants were grown under two temperature regimes: control conditions (32 °C day/25 °C night; 12 h each) and heat stress conditions (42 °C day/30 °C night; 12 h each). Seeds were sown in 20 cm diameter pots filled with potting soil (“Fafard® 3B Mix/Metro-Mix® 830; SUNGRO Horticulture, Agawam, MA, USA”). Three biological replicates were used for each genotype, with each replicate consisting of three plants. At maturity, three seeds per plant were randomly harvested for subsequent metabolomic analysis.

In the growth chamber, photosynthetically active radiation (400–700 nm) was maintained at 600 $\mu\text{mol m}^{-2} \text{ s}^{-1}$ using cool fluorescent lamps, with a 12 h photoperiod and an average relative humidity of 60%². Plants were watered regularly to maintain field capacity (moist but without runoff) and fertilized every 7–14 days with $\frac{1}{2}$ teaspoon of Miracle-Gro (24-8-16) per 4.5 L of water^{2,9}. Temperature data were recorded using a HOBO® data logger (Onset Computer Corporation, USA), as shown in Fig. S1.

Metabolite extraction

Physiologically mature mung bean seeds were thawed on ice, and 100 mg of each sample was transferred into 2 mL microcentrifuge tubes. Metabolites were extracted with 800 μL of 80% methanol and ground at 65 Hz for 180 s. The homogenized samples were vortexed and sonicated for 30 min at 4 °C (for details see Jha et al.²⁶).

Samples were stored at –20 °C for 1 h, vortexed for 30 s, incubated at 4 °C for 30 min, centrifuged at 12,000 rpm for 15 min at 4 °C, and the supernatant was collected. The supernatant was stored at –20 °C for 1 h before centrifuging at 12,000 rpm for 15 min at 4 °C²⁶. Finally, 200 μL of the resulting supernatant and 5 μL of DL-*o*-chlorophenylalanine (0.14 mg/mL) were transferred into vials for LC–MS analysis^{28,29}.

Ultra-high-performance liquid chromatography–mass spectrometry (UHPLC–MS) analysis

Metabolite profiling was performed using an ACQUITY Ultra-Performance Liquid Chromatography (UPLC) system (Waters, Milford, MA, USA) coupled to a Q Exactive™ Orbitrap high-resolution mass spectrometer (Thermo Fisher Scientific, Bremen, Germany) equipped with a heated electrospray ionization (HESI) source. This platform enabled high-resolution, high-mass-accuracy detection of a broad range of primary and secondary metabolites.

Chromatographic separation was achieved on an ACQUITY UPLC HSS T3 reversed-phase column (100 \times 2.1 mm, 1.8 μm particle size), which is optimized for the retention and resolution of both polar and moderately non-polar metabolites. The column temperature was maintained at 40 °C to ensure reproducible retention times and optimal peak shapes, while the autosampler temperature was set at 4 °C to prevent metabolite degradation during analysis.

A binary solvent system was employed, consisting of 0.05% (v/v) formic acid in ultrapure water as mobile phase A and acetonitrile as mobile phase B. Metabolites were eluted using a linear gradient program designed to maximize metabolome coverage: 0–1 min, 5% B; 1–12 min, 5–95% B; 12–13.5 min, 95% B; 13.5–13.6 min, 95–5% B; and 13.6–16 min, 5% B for column re-equilibration. The flow rate was maintained at 0.3 mL min^{–1}, ensuring efficient separation with minimal backpressure. This chromatographic method was adapted from previously optimized protocols (Jha et al.²⁶).

Mass spectrometry conditions

Mass spectrometric data acquisition was carried out in both positive (ESI⁺) and negative (ESI[–]) ionization modes to enhance metabolite coverage, as different chemical classes preferentially ionize under different polarity conditions. The mass spectrometer was operated in full-scan mode with high mass accuracy, allowing reliable metabolite detection and annotation.

For ESI⁺ mode, the ion source parameters were set as follows: heater temperature 300 °C, sheath gas flow 45 arbitrary units (arb), auxiliary gas flow 15 arb, sweep gas flow 1 arb, spray voltage 3.0 kV, capillary temperature 350 °C, and S-lens RF level 30%.

For ESI⁻ mode, the corresponding parameters were: heater temperature 300 °C, sheath gas flow 45 arb, auxiliary gas flow 15 arb, sweep gas flow 1 arb, spray voltage 3.2 kV, capillary temperature 350 °C, and S-lens RF level 60%. These optimized conditions ensured efficient ionization, reduced in-source fragmentation, and improved sensitivity across diverse metabolite classes²⁶.

Together, this UHPLC–MS workflow provided high chromatographic resolution and accurate mass detection, enabling robust, reproducible, and comprehensive metabolomic profiling suitable for downstream statistical and biological interpretation.

Statistical analysis

Raw data acquisition and alignment were performed in Compound Discoverer (v3.0, Thermo) using *m/z* values and retention times. Data from both ionization modes were merged and imported into SIMCA-P (v14.1) for multivariate analysis²⁷. Principal component analysis (PCA) was first used as an unsupervised method for visualizing sample clustering and detecting outliers³⁰. Supervised models, including partial least squares discriminant analysis (PLS-DA)³¹ and orthogonal PLS-DA (OPLS-DA), were then applied to identify potential biomarkers. Candidate metabolites were screened using a variable importance in projection (VIP)³² score > 1.5 and a fold-change (FC) threshold $|\log_2\text{FC}| > 1$. Metabolites with $\log_2\text{FC} \geq 1$ (upregulated) or ≤ -1 (downregulated) and $P < 0.05$ were considered significantly differentially expressed.

Metabolite identification

Key metabolites were identified by matching precise mass and MS/MS fragmentation data against publicly available databases, including the Human Metabolome Database (HMDB; www.hmdb.ca), ChemSpider (www.chemspider.com), and MassBank (www.massbank.jp). When necessary, metabolite identities were confirmed using authentic standards based on retention times and MS/MS fragmentation patterns²⁶.

Cluster analysis

Hierarchical clustering analysis (HCA) was performed using the complete linkage algorithm in Cluster 3.0 (Stanford University), and visualized using the *heatmap* “R package (version 1.0.12, Raivo Kolde). The HCA was based on metabolite ratios from two experimental conditions, highlighting significantly altered metabolites. In the heatmaps, red and green represent metabolite levels higher or lower than the mean, respectively.

Metabolite correlation network and pathway enrichment

A metabolite correlation network was constructed using KEGG pathway data^{33,34} integrated with the MetaboAnalyst platform to explore functional associations among significantly altered metabolites ($P < 0.05$). Key metabolites were annotated through HMDB and KEGG to identify related pathways, enzymes, and biological functions. Enriched pathways were visualized using dot plots and network diagrams to illustrate the interconnected roles of crucial biomarkers involved in the heat stress response²⁶.

Results and discussion

Phenotypic performance of contrasting genotypes under control and heat stress

Under control condition (32 °C day/25 °C night), the heat-tolerant mung bean genotype PI425243 exhibited significantly superior reproductive performance compared with the heat-sensitive genotype PI223002, producing higher numbers of effective pods per plant (EPPP; 25 vs. 21), seeds per plant (SPP; 150 vs. 138), and seed yield per plant (SYPP; 6.6 g vs. 6.1 g) (Fig. 1). These differences, though moderate under optimal conditions, indicate inherent genotypic variation in yield-related traits. Additional morpho-physiological parameters are presented in Table 1.

Exposure to heat stress (42 °C day/30 °C night) markedly reduced reproductive output in both genotypes; however, PI425243 maintained significantly higher productivity than PI223002. Under heat stress, PI425243 produced 10 EPPP and 40 SPP, whereas PI223002 produced only 6 EPPP and 24 SPP (Fig. 1). Correspondingly, SYPP was significantly higher in PI425243 (4.6 g) than in PI223002 (2.9 g), confirming its superior heat tolerance. These results are consistent with earlier reports demonstrating that elevated temperatures severely impair reproductive development and yield in mung bean and other grain legumes, with tolerant genotypes showing greater yield stability under stress^{2,10}.

Multivariate metabolomic analysis reveals genotype-specific metabolic reprogramming

To investigate global metabolic variations among samples, principal component analysis (PCA) was first performed using data acquired from both ionization modes. PCA is an unsupervised multivariate technique that highlights intrinsic variation and enables visualization of overall metabolic patterns. PCA revealed a clear separation between PI425243 and PI223002 under control and heat stress conditions (Fig. 2a, d), indicating distinct metabolite profiles associated with genotype and thermal regime. To enhance group discrimination and reduce nonspecific variation, supervised models including PLS-DA and OPLS-DA were employed. Both models showed strong separation between genotypes under control (Fig. 2b, e) and heat stress (Fig. 2c, f), reflecting robust genotype-dependent metabolic reprogramming in response to heat.

Metabolites contributing most strongly to genotype discrimination were identified using a VIP score > 1.5. Score and loading plots (Fig. 3a–c under non stress) and (Fig. 3b–d under heat stress) highlighted key metabolites responsible for separation, suggesting that specific secondary metabolites play central roles in conferring heat tolerance. Similar study has been reported in chickpea seed metabolomics assessed under heat stress condition²⁶.

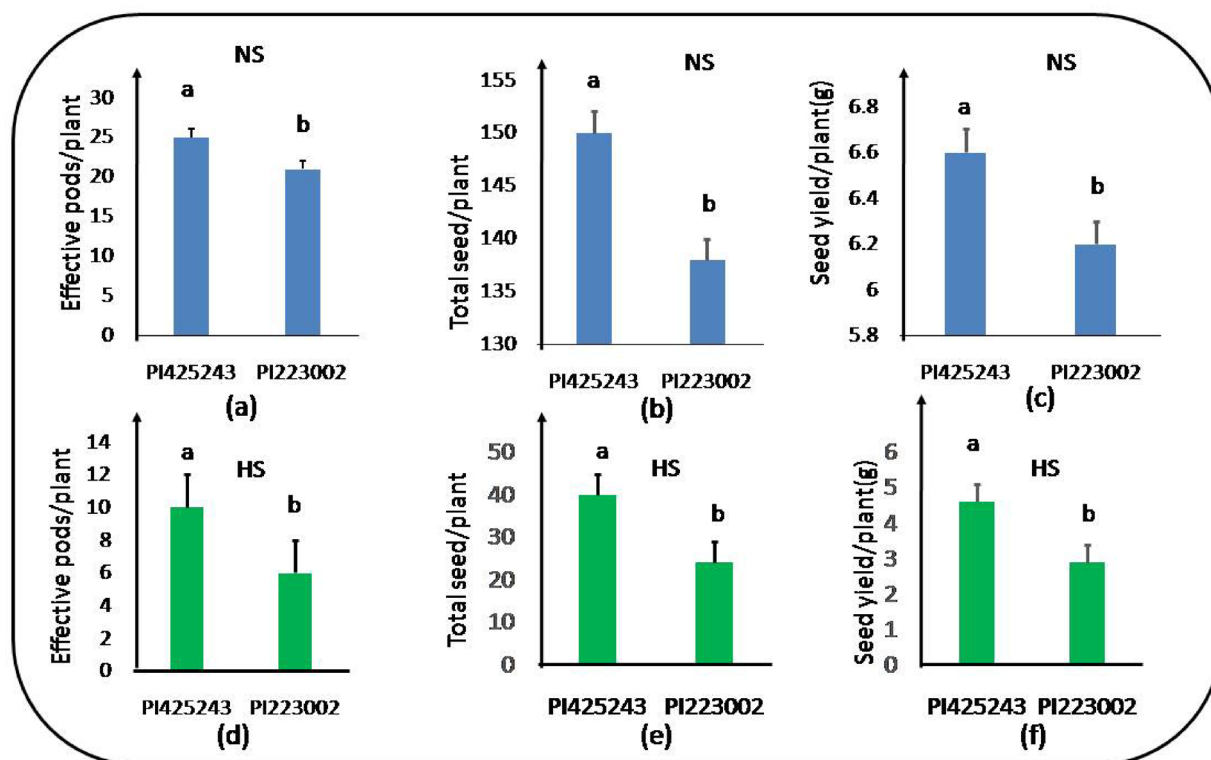


Fig. 1. Yield parameters of mung bean genotypes PI425243 (heat tolerant) and PI223002 (heat sensitive) under non stress (NS) and heat stress (HS) conditions. Performance under NS (32°/25 °C): (a) effective pods/plant, (b) total seeds/plant, and (c) seed yield per plant. Performance under HS (42°/30 °C): (d) effective pods/plant, (e) total seeds/plant, and (f) seed yield/plant. Values represent means + SE (n = 5). Different lowercase letters above bars indicate significant differences between genotypes within a treatment at $P < 0.05$ according to Tukey's Honest Significant Difference (HSD) test.

| Genotype | Days to first flowering | Days to first podding | Plant height(cm) | Days to maturity | Total effective pods/plant | Total seeds/plant | Seed yield/plant(g) |
|---|-------------------------|-----------------------|------------------|------------------|----------------------------|-------------------|---------------------|
| Morpho- physiological traits of contrasting genotypes under non stress condition | | | | | | | |
| PI425243 | 43 | 53 | 55.5 | 67 | 25 | 150 | 6.6 |
| PI223002 | 45 | 54 | 44.1 | 68 | 21 | 138 | 6.1 |
| Morpho- physiological traits of contrasting genotypes under heat stress condition | | | | | | | |
| PI425243 | 39 | 45 | 48.5 | 58 | 10 | 40 | 4.6 |
| PI223002 | 32 | 40 | 34.8 | 53 | 6 | 24 | 2.9 |

Table 1. Mean value of morpho-physiological traits of contrasting genotypes under non stress and heat stress condition.

Differential metabolite accumulation under control (non stress) and heat stress

Single-variable analysis using volcano plots revealed substantial differences in metabolite abundance between the two genotypes. Under control conditions, 87 metabolites were differentially accumulated in PI425243 relative to PI223002, with 55 upregulated and 32 downregulated (Fig. 4a). Under heat stress, 68 metabolites showed differential accumulation, including 39 upregulated and 29 downregulated metabolites in PI425243 (Fig. 4b).

Notably, under control conditions, PI425243 showed significantly higher accumulation of several phenolic acids and flavonoids, including hydrocinnamic acid [Fold change (FC)=6.03], 5-hydroxyferulic acid (FC = 11.75), luteolin 7-malonylglucoside (FC=4.28), quercetin 3-(6"-malonyl-glucoside) (FC=5.89), and kaempferol 3-(2G--apiosylrobinobioside) (FC=8.19) (Tables 2 and S1). In contrast, metabolites such as diosmin (FC = -9.92), naringin (FC = -6.63), rhoifolin (FC = -7.25), pinocembrin 7-rhamnosylglucoside (FC = -3.96), and rubraflavone D (FC = -4.57) were more abundant in the heat-sensitive genotype PI223002, particularly under heat stress. Similarly, metabolomics analysis resulted in high accumulation of various flavonoids in chickpea seeds²⁶.

Under heat stress, 68 metabolites were differentially accumulated, with 39 upregulated and 29 downregulated in PI425243. Notable upregulated metabolites included hydrocinnamic acid (FC = 4.46), 5-hydroxyferulic acid (FC = 13.1), quercetin (FC = 2.3), myricetin (FC = 4.2), and kaempferol 3-(2G--apiosylrobinobioside) (FC = 8.66).

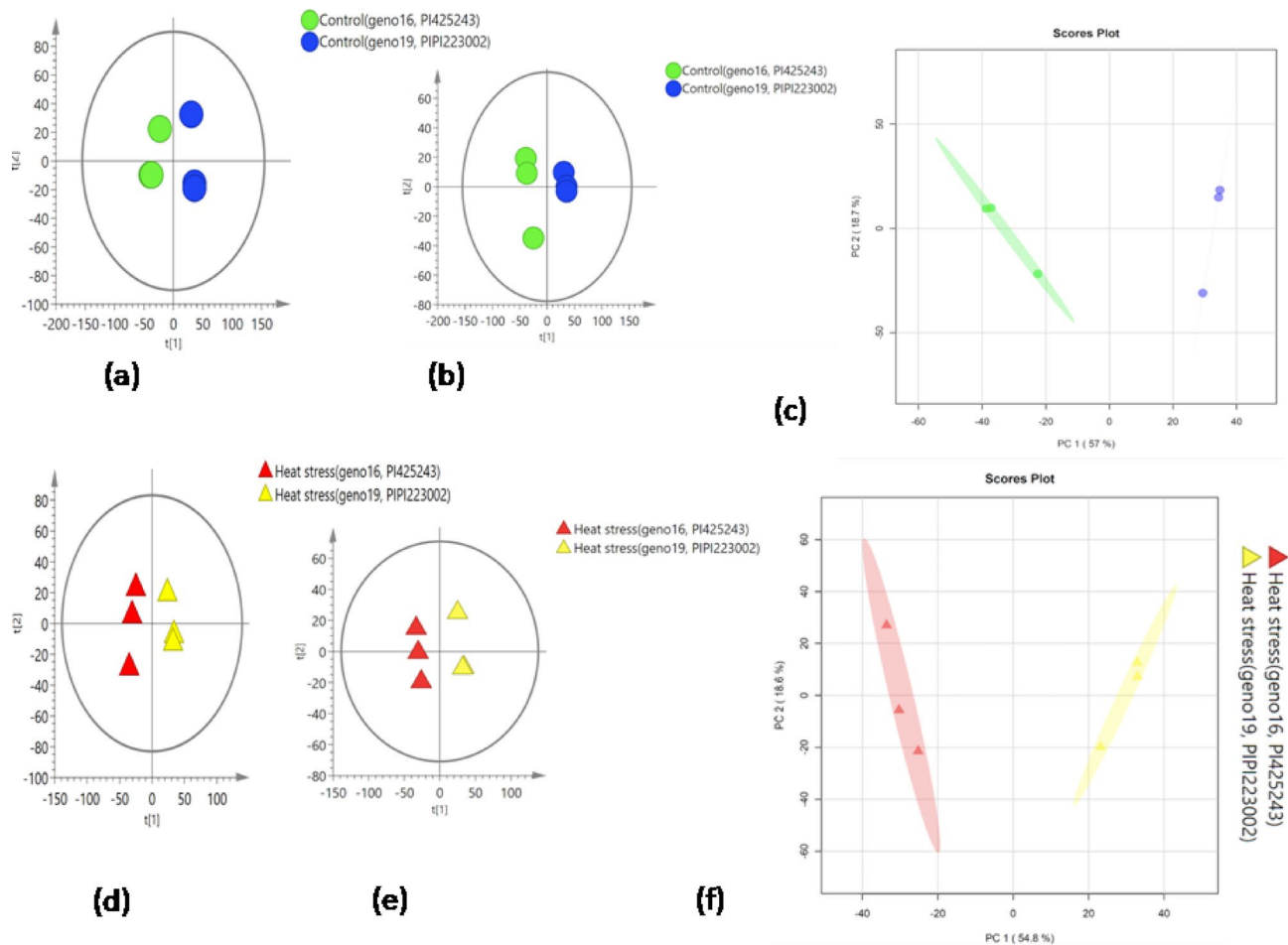


Fig. 2. Multivariate analysis of metabolites under non-stress and heat stress conditions in mung bean genotypes. **(a, d)** PCA score scatter plot under non-stress and heat stress; **(b, e)** PLS-DA score scatter plot non-stress and heat stress; **(c, f)** OPLS-DA score scatter plot non-stress and heat stress.

The most significantly downregulated metabolites were oleanolic acid (FC = -2.04), naringin (FC = -4.8), diosmin (FC = -9.1), rhoifolin (FC = -4.9), and goshonoside F7 (FC = -5.7) (Tables 3 and S2).

Hierarchical clustering analysis further confirmed clear genotype-specific metabolic signatures under heat stress (Fig. 5). PI425243 clustered separately from PI223002 and was characterized by higher accumulation of metabolites including hydrocinnamic acid, 5-hydroxyferulic acid, quercetin, myricetin, kaempferol 3-(2G-apiosylrobinobioside), and hesperetin 7-neohesperidoside with known antioxidant and stress-protective functions, suggesting their potential as biochemical markers for heat tolerance.

Flavonoids as central mediators of heat stress tolerance

Flavonoids constitute a major class of plant secondary metabolites with well-established roles in mitigating oxidative stress through ROS scavenging^{35–37}. In the present study, heat tolerance in PI425243 was strongly associated with increased accumulation of flavonols such as kaempferol, quercetin, and myricetin under heat stress. These compounds are known to interact with ABA and auxin signaling pathways, regulate stomatal behavior, and enhance antioxidant enzyme activities, thereby maintaining cellular redox homeostasis under stress.

Kaempferol and quercetin have been widely implicated in tolerance to drought, salinity, and heat stress across multiple crop species, including chickpea, rice, maize, and tomato^{38–41}. Their enhanced accumulation in PI425243 likely contributes to improved protection of photosynthetic machinery and reproductive tissues under high temperature. Similarly, increased myricetin accumulation may further strengthen antioxidant capacity, as reported previously in heat-tolerant rice, maize and tomato genotypes^{42–44}.

Interestingly, naringin and diosmin—flavonoids often associated with stress protection^{45–47}—were more abundant in the heat-sensitive genotype PI223002 under heat stress. This suggests that their accumulation alone may not be sufficient to confer heat tolerance and may instead reflect a stress-induced metabolic imbalance rather than an adaptive response.

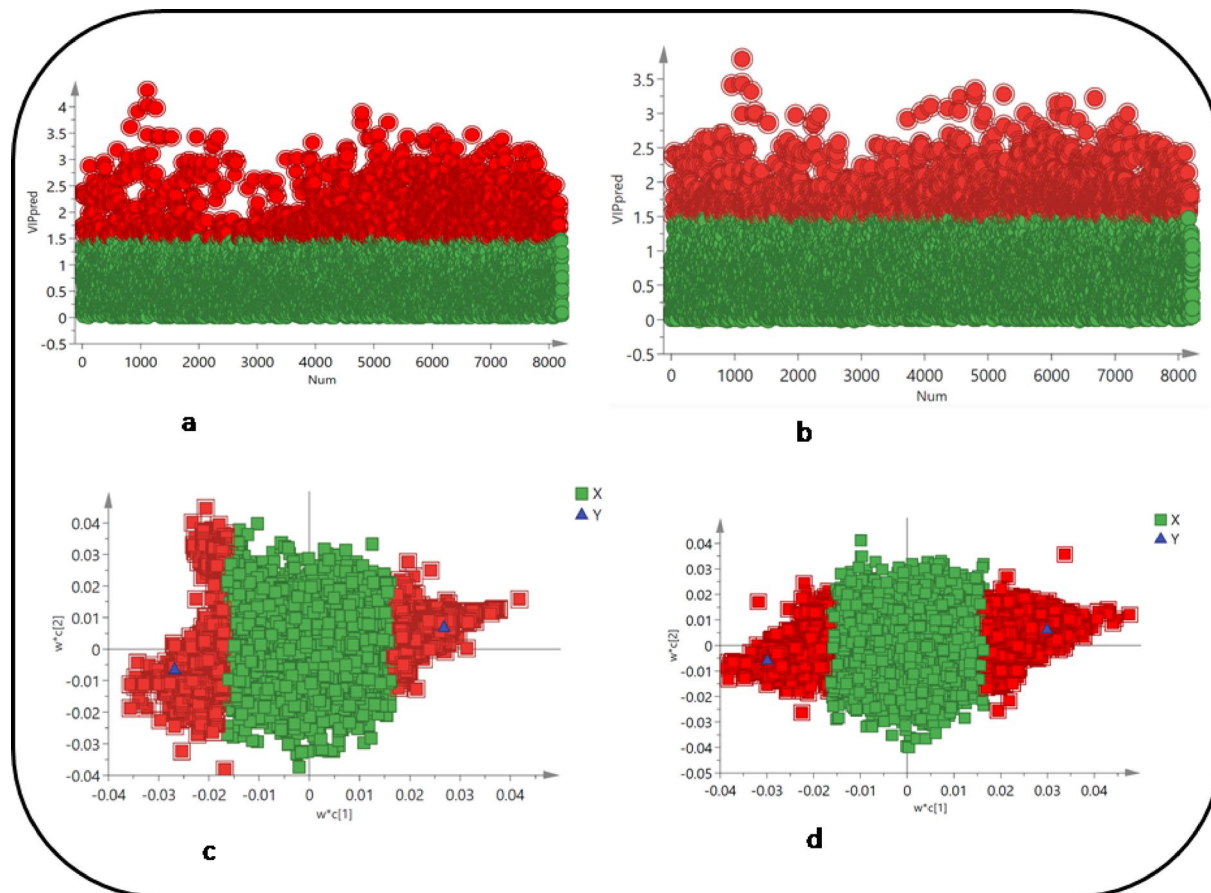


Fig. 3. Distribution and significance of metabolites in mung bean genotypes. (a) VIP values (VIP > 1.5) under non-stress; (b) VIP values (VIP > 1.5) under heat stress; (c) PLS-DA loading plot under non stress, significant metabolites (VIP > 1.5) highlighted in red boxes; (d) PLS-DA loading plot under heat stress, significant metabolites (VIP > 1.5) highlighted in red boxes.

Phenolic acids as metabolic signatures of heat stress response in mungbean seeds

Hydroxycinnamic acids (HCAs), including *p*-coumaric, caffeic, ferulic, and sinapic acids, along with their conjugates such as chlorogenic acid, are central intermediates in plant metabolism⁴⁸.

Hydroxycinnamic acids, including hydrocinnamic acid and ferulic acid derivatives, were significantly enriched in PI425243 under heat stress. These compounds are central intermediates in phenylpropanoid metabolism and play key roles in lignin biosynthesis, membrane stabilization, and antioxidant defense^{49,50}.

Ferulic acid, a phenolic acid derived from cinnamic acid, plays diverse roles in plant responses to both biotic and abiotic stresses⁵¹. It is well-established as a protective compound against heat stress⁵². Ferulic acid and its derivatives have been shown to enhance heat tolerance by upregulating antioxidant enzymes, increasing osmolyte accumulation, and preserving photosynthetic efficiency⁵¹. The elevated levels of 5-hydroxyferulic acid observed in PI425243 likely contribute to enhanced ROS detoxification and structural integrity under heat stress, consistent with reports in maize, barley (*Hordeum vulgare*), tomato (*Solanum lycopersicum*), and blueberry (*Vaccinium corymbosum*)^{51–54}.

Terpenoids exhibit genotype-specific responses to heat stress

Terpenoids, also known as isoprenoids, represent the largest class of specialized plant metabolites⁵⁵ and play pivotal roles in plant growth, survival, and defense⁵⁶. More broadly, terpenoids have been implicated in enhancing tolerance to various stresses, including heat^{57,58}. For example, in tomato, exposure to 37 °C increased emissions of several monoterpenes, such as 2-carene, α -phellandrene, limonene, and β -phellandrene, whereas elevated α -pinene was detected only at temperatures ≥ 46 °C⁵⁷. The monoterpene (E)- β -ocimene was observed exclusively at ≥ 46 °C⁵⁷. Furthermore, heat-tolerant tomato genotypes, such as IHR-2841, exhibited a two-fold induction of terpenoid synthase genes under heat stress, with the enhanced expression of β -caryophyllene synthase (TPS12) and β -phyllandrene synthase (TPS20) linked to heat tolerance⁵⁹. Heat stress responses also vary across species. For instance, at 49 °C, *Amaranthus cruentus*, *A. hybridus*, *Solanum aethiopicum*, *Telfairia occidentalis*, and *Vigna unguiculata* exhibited species-specific terpenoid emissions, with higher constitutive isoprenoid emission correlating with greater heat tolerance, whereas less resistant species displayed stronger stress-induced terpenoid induction⁶⁰.

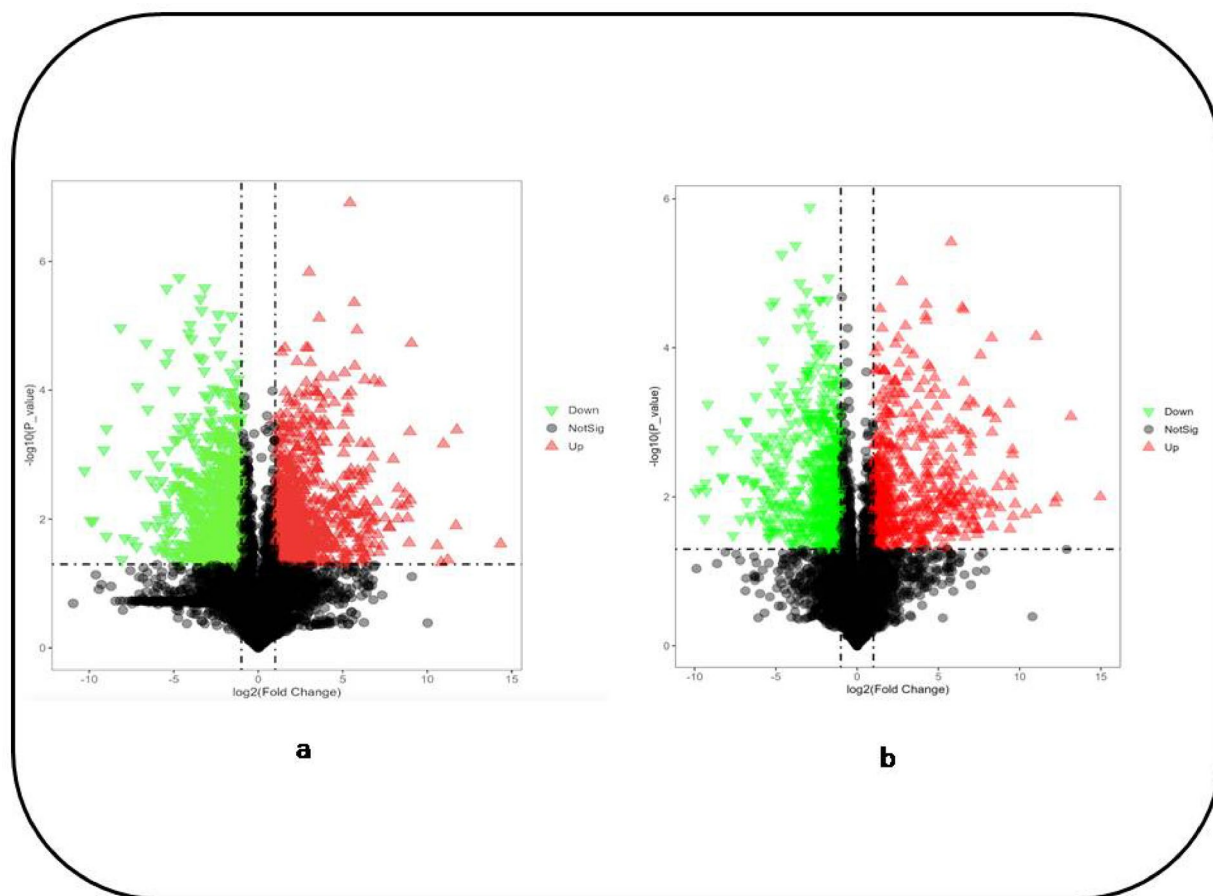


Fig. 4. Volcano plots of differentially expressed metabolites in PI425243 vs PI 223002. **(a)** Non-stress condition: red, upregulated; green, downregulated; gray, no change. **(b)** Heat-stress condition: red, upregulated; green, downregulated; gray, no change.

| Serial no. | RT [min] | Molecular weight | m/z | HMDB_ID | Compound name | Chemical formula | Log2(FC) | T-test | VIP | Regulation |
|------------|----------|------------------|----------|-------------|--|------------------|----------|--------|-----|------------|
| 1 | 3.826 | 150.0682 | 149.0609 | HMDB0000764 | Hydrocinnamic acid | C9H10O2 | 6.03 | 0.020 | 2.4 | UR |
| 2 | 2.408 | – | 255.0508 | HMDB0035484 | 5-Hydroxyferulic acid | C10H10O5 | 11.75 | 0.010 | 3.4 | UR |
| 3 | 3.742 | – | 515.0807 | HMDB0301681 | Luteolin 7-malonylglucoside | C24H22O14 | 4.28 | 0.032 | 2.1 | UR |
| 4 | 1.738 | 550.0932 | 549.0859 | HMDB0037368 | Quercetin 3-(6"-malonyl-glycoside) | C24H22O15 | 5.89 | 0.019 | 2.4 | UR |
| 5 | 3.839 | – | 707.1853 | HMDB0039759 | Kaempferol 3-(2G-apiosylrobinobioside) | C32H38O19 | 8.19 | 0.032 | 2.9 | UR |
| 6 | 5.894 | 608.1744 | 607.1671 | HMDB0029548 | Diosmin | C28H32O15 | –9.92 | 0.039 | 3.1 | DR |
| 7 | 5.976 | 580.1798 | 579.1725 | HMDB0002927 | Naringin | C27H32O14 | –6.63 | 0.003 | 2.6 | DR |
| 8 | 5.34 | 578.1643 | 577.157 | HMDB0038848 | Rhoifolin | C27H30O14 | –7.25 | 0.020 | 2.7 | DR |
| 9 | 6.896 | – | 599.1547 | CSID390892 | Pinocembrin 7-rhamnosylglucoside | C27H32O13 | –3.96 | 0.020 | 2.0 | DR |
| 10 | 4.686 | – | 533.2234 | HMDB0030631 | Rubraflavone D | C30H32O6 | –4.57 | 0.027 | 2.1 | DR |

Table 2. Selected differentially expressed metabolite in mung bean seeds of PI425243 compared to PI223002 under non stress conditions. UR: upregulated; DR: downregulated.

In the present study, oleanolic acid, a pentacyclic triterpenoid, accumulated to higher levels in the heat-sensitive genotype PI223002 under heat stress. While terpenoids have been associated with stress tolerance in several species, this contrasting pattern suggests that terpenoid-mediated heat adaptation in mung bean may involve complex, genotype-specific regulatory mechanisms rather than a simple positive correlation with tolerance.

Pathway-level insights into heat stress adaptation

KEGG pathway enrichment analysis revealed that differentially accumulated metabolites were significantly associated with starch and sucrose metabolism, tyrosine metabolism under control condition and starch and

| Serial no. | RT [min] | Molecular weight | m/z | HMDB_ID | Compound name | Chemical formula | Log2(FC) | T-test | VIP | Regulation |
|------------|----------|------------------|-----------|-------------|---|------------------|----------|--------|------|------------|
| 1 | 3.826 | 150.06815 | 149.06088 | HMDB0000764 | Hydrocinnamic acid | C9H10O2 | 4.460 | 0.04 | 2.36 | UR |
| 2 | 2.408 | – | 255.05084 | HMDB0035484 | 5-Hydroxyferulic acid | C10H10O5 | 13.160 | 0.02 | 4.03 | UR |
| 3 | 6.304 | 302.0428 | 301.03552 | HMDB0005794 | Quercetin | C15H10O7 | 2.332 | 0.01 | 1.69 | UR |
| 4 | 6.212 | 318.03786 | 317.03058 | HMDB0002755 | Myricetin | C15H10O8 | 4.249 | 0.04 | 2.32 | UR |
| 5 | 3.839 | – | 707.18529 | HMDB0039759 | Kaempferol 3-(2G- <i>apiosylrobinobioside</i>) | C32H38O19 | 8.622 | 0.05 | 3.27 | UR |
| 6 | 12.626 | 456.36019 | 455.35291 | HMDB0002364 | Oleanolic acid | C30H48O3 | –2.043 | 0.02 | 1.57 | DR |
| 7 | 5.976 | 580.17977 | 579.17249 | HMDB0002927 | Naringin | C27H32O14 | –4.841 | 0.05 | 2.48 | DR |
| 8 | 5.894 | 608.17435 | 607.16707 | HMDB0029548 | Diosmin | C28H32O15 | –9.198 | 0.02 | 3.37 | DR |
| 9 | 5.409 | 578.1629 | 579.17034 | HMDB0038848 | Rhoifolin | C27H30O14 | –4.948 | 0.033 | 3.09 | DR |
| 10 | 7.317 | – | 675.36294 | HMDB0038378 | Goshonoside F7 | C32H54O12 | –5.758 | 0.01 | 2.67 | DR |

Table 3. Selected differentially expressed metabolite in mung bean seeds of PI425243 compared to PI223002 under heat stress conditions. UR: upregulated; DR:downregulated.

sucrose metabolism and terpenoid biosynthesis under heat stress. Disruption of starch biosynthesis under heat stress is well documented and often leads to reduced assimilate availability during grain filling^{61–64}. The enrichment of carbohydrate metabolism pathways in PI425243 suggests improved metabolic flexibility and energy homeostasis under heat stress.

Tyrosine metabolism and steroid hormone biosynthesis

Heat stress induces extensive metabolic and hormonal reprogramming, with tyrosine metabolism and steroid hormone biosynthesis emerging as key pathways associated with thermotolerance. Tyrosine-derived metabolites, including the thermomemory compound salidroside⁶⁵, contribute to heat stress acclimation and oxidative stress mitigation, as demonstrated across diverse plant systems, while elevated tyrosine levels may directly scavenge reactive oxygen species⁶⁶. Although caffeine biosynthesis is limited to a few plant species, evidence from rice suggests a potential role in abiotic stress tolerance through Ca²⁺-dependent protein kinase signaling^{67,68}. In parallel, brassinosteroids play a central role in heat stress tolerance by activating HsfA1d-mediated transcription, enhancing ethylene biosynthesis, and strengthening cellular defense mechanisms^{69,70}. Consistent improvements in growth, yield, and antioxidant capacity following exogenous brassinosteroid application across crops further support the involvement of steroid hormone signaling in thermotolerance^{71–73}. Collectively, these findings highlight tyrosine-associated metabolic pathways and steroid hormone biosynthesis as plausible molecular mechanisms underlying heat tolerance in mung bean.

Implications for heat tolerance breeding in mung bean

Collectively, these results demonstrate that heat tolerance in mung bean is associated with coordinated metabolic reprogramming, particularly involving flavonoids, phenolic acids, and hormone-related pathways (see Fig. 6). The consistent enrichment of kaempferol, quercetin, myricetin, hydrocinnamic acid, and 5-hydroxyferulic acid in the heat-tolerant genotype PI425243 highlights their potential as metabolic biomarkers for heat tolerance. These findings provide valuable biochemical insights that can be integrated with genetic and genomic approaches to accelerate the development of heat-resilient mung bean cultivars.

Conclusion

The increasing frequency and intensity of heat stress driven by climate change pose a significant threat to mungbean productivity and global food security. This study provides metabolomics-based evidence that seed traits are highly responsive to heat stress and identifies specific metabolites—hydroxycinnamic acid, 5-hydroxyferulic acid, quercetin, myricetin, kaempferol 3-(2G-*apiosylrobinobioside*), and hesperetin 7-*neohesperidoside*—as key biochemical signatures associated with heat tolerance in mungbean. In addition, the involvement of starch and sugar metabolism, tyrosine metabolism, caffeine metabolism, and steroid hormone biosynthesis highlights coordinated metabolic adjustments underlying thermal resilience. Collectively, these findings document seed metabolic signatures associated with heat stress tolerance, while acknowledging that functional validation is required to establish causal or mechanistic links. The identified metabolites and pathways nonetheless offer promising biomarkers for seed-based selection and metabolite-assisted breeding of climate-resilient mungbean.

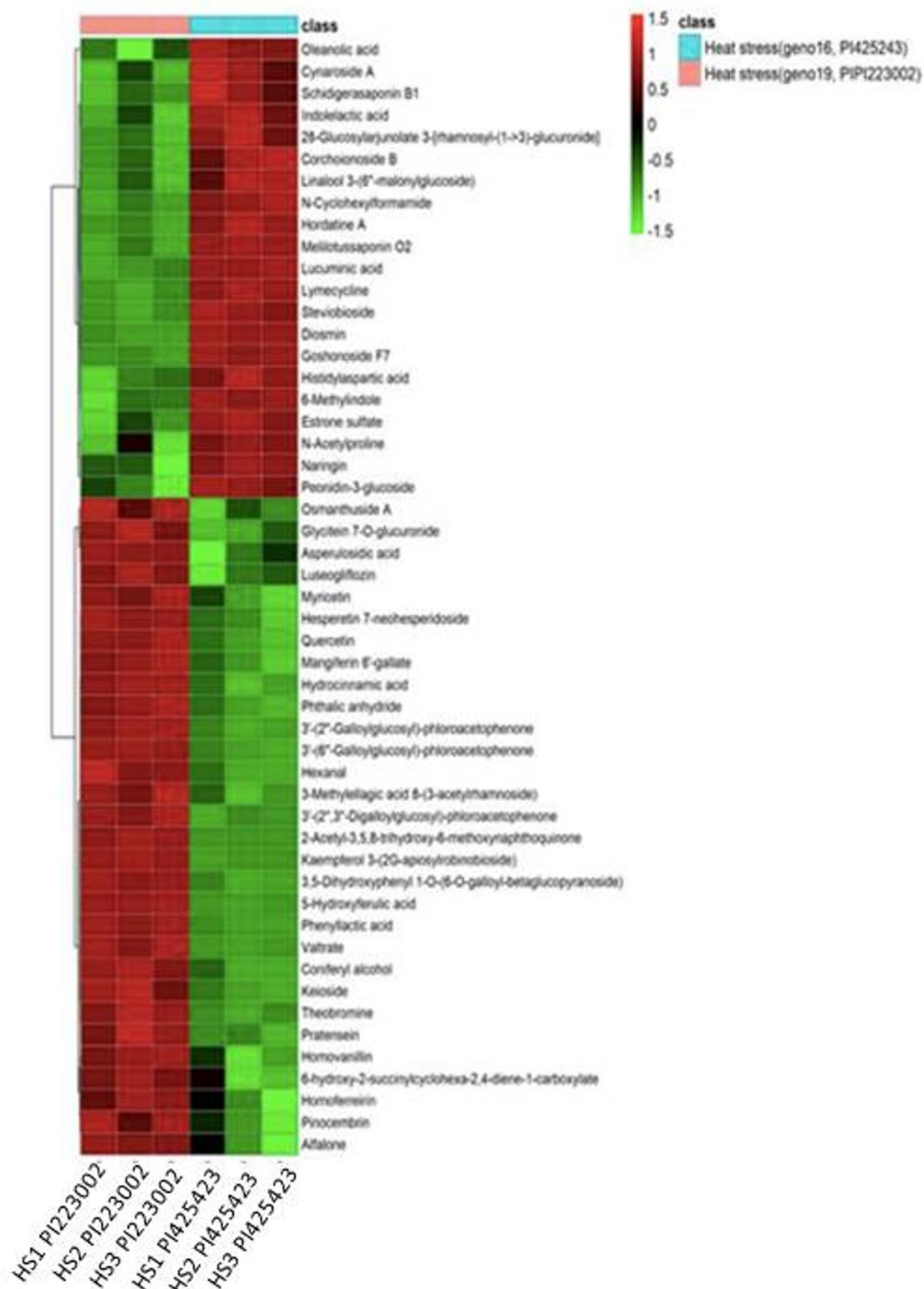


Fig. 5. Heat map and hierarchical cluster analysis of significant metabolites under heat stress. PI425243 and PI223002 were clearly separated, with PI425243 showing higher accumulation of potential biomarker metabolites, including hydrocinnamic acid, 5-hydroxyferulic acid, quercetin, myricetin, kaempferol 3-(2G-apiosylrobinobioside), and hesperetin 7-neohesperidoside.

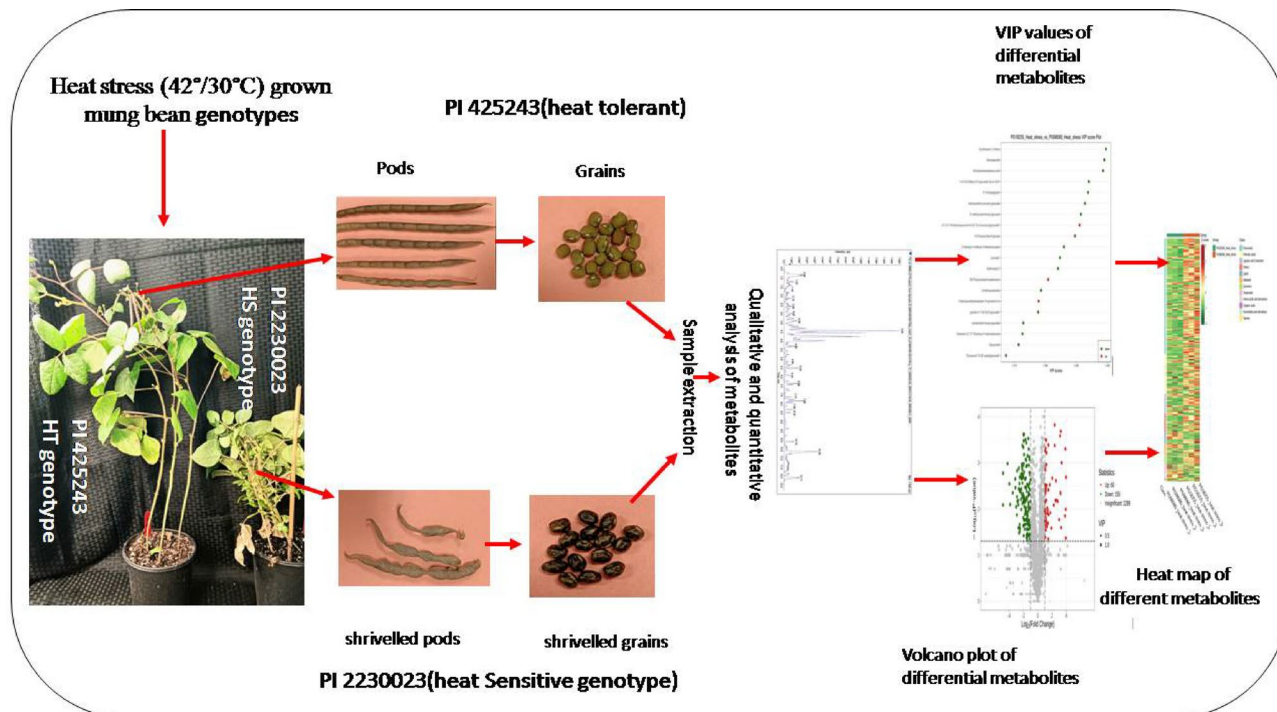


Fig. 6. Experimental workflow and comparative metabolomic profiling of heat-tolerant and heat-sensitive mung bean genotypes under heat stress. Plants were grown under heat stress conditions (42°/30 °C), comparing the heat-tolerant genotype PI 425243 with the heat-sensitive genotype PI 2230023. Heat stress resulted in normal pod and grain development in the tolerant genotype, whereas the sensitive genotype exhibited shriveled pods and grains. Grains were subjected to metabolite extraction followed by qualitative and quantitative metabolite analysis. Multivariate and univariate analyses identified heat-responsive differential metabolites, visualized through VIP score plots, volcano plots, and heat maps, highlighting metabolic differences associated with heat tolerance.

Data availability

The original contributions presented in this study are included in the article and/or supplementary material. Further inquiries can be directed to the corresponding author/s.

Received: 22 November 2025; Accepted: 12 February 2026

Published online: 23 March 2026

References

- Hou, D. et al. Mungbean (*Vigna radiata* L.): Bioactive polyphenols, polysaccharides, peptides, and health benefits. *Nutrients* **11**(6), 1238 (2019).
- Jha, U. C. et al. Dynamic changes in seed nutritional components of mung bean [(*Vigna radiata* (L.) R. Wilczek)] under heat stress. *Sci. Rep.* **15**, 12586 (2025).
- Nair, R. M. et al. Biofortification of mungbean (*Vigna radiata*) as a whole food to enhance human health. *J. Sci. Food Agric.* **93**, 1805–1813 (2013).
- Nair, R. M. et al. *The Mungbean Genome*. (Springer, 2020) <https://doi.org/10.1007/978-3-030-20008-4>.
- Ilyas, N. et al. Contribution of nitrogen fixed by mung bean to the following wheat crop. *Commun. Soil Sci. Plant Anal.* **49**(2), 148–158 (2018).
- Yaqub, M. et al. Induction of mungbean [*Vigna radiata* (L.) Wilczek] as a grain legume in the annual rice-wheat double cropping system. *Pak. J. Bot.* **42**, 3125–3135 (2010).
- Jha, U. C. et al. Heat stress in crop plants: Its nature, impacts and integrated breeding strategies to improve heat tolerance. *Plant Breed.* **133**(6), 679–701 (2014).
- Van Haeften, S. et al. Building a better mungbean: Breeding for reproductive resilience in a changing climate. *Food Energy Secur.* **12**(6), e467 (2023).
- Jha, U. C. et al. Differential physiological and yield responses of selected mung bean (*Vigna radiata* (L.) R. Wilczek) genotypes to various high-temperature stress regimes. *Sci. Rep.* **15**(1), 1034. <https://doi.org/10.1038/s41598-024-84615-6> (2025).
- Priya, M. et al. Investigating the influence of elevated temperature on nutritional and yield characteristics of mung bean (*Vigna radiata* L.) genotypes during seed filling in a controlled environment. *Front. Plant Sci.* **14**, 1233954 (2023).
- Lawas, L. M. F. et al. Metabolic responses of rice cultivars with different tolerance to combined drought and heat stress under field conditions. *Gigascience* **8**(5), giz050. <https://doi.org/10.1093/gigascience/giz050> (2019).
- Zhao, P. et al. Integrated transcriptomics and metabolomics analysis of two maize hybrids (ZD309 and XY335) under heat stress at the flowering stage. *Genes* **15**(2), 189 (2024).
- Zhou, J. et al. Comparative transcriptomic and metabolomic analyses provide insights into the responses to high temperature stress in Alfalfa (*Medicago sativa* L.). *BMC Plant Biol.* **24**(1), 776 (2024).

14. Da Costa, M. V. J. et al. Comparative metabolite profiling of rice contrasts reveal combined drought and heat stress signatures in flag leaf and spikelets. *Plant Sci.* **320**, 111262 (2022).
15. Mishra, A. et al. Effect of high temperature stress on metabolome and aroma in rice grains. *Plant Gene* **38**, 100450 (2024).
16. Christensen, S. A. et al. Metabolomics by UHPLC-HRMS reveals the impact of heat stress on pathogen-elicited immunity in maize. *Metabolomics* **17**, 1–11 (2021).
17. Li, H. et al. Metabolomic and transcriptomic analyses reveal that sucrose synthase regulates maize pollen viability under heat and drought stress. *Ecotoxicol. Environ. Saf.* **246**, 114191 (2022).
18. Liu, J. et al. Uncovering the gene regulatory network of maize hybrid ZD309 under heat stress by transcriptomic and metabolomic analysis. *Plants* **11**(5), 677 (2022).
19. Abdelrahman, M. et al. Heat stress effects on source–sink relationships and metabolome dynamics in wheat. *J. Exp. Bot.* **71**(2), 543–554 (2020).
20. Matsunaga, S. et al. Metabolome profiling of heat priming effects, senescence, and acclimation of bread wheat induced by high temperatures at different growth stages. *Int. J. Mol. Sci.* **22**(23), 13139 (2021).
21. Shunkao, S. et al. Integrative physiological and metabolomics study reveals adaptive strategies of wheat seedlings to salt and heat stress combination. *Plant Growth Regul.* **100**(1), 181–196 (2023).
22. Ma, D. et al. Metabolomics and transcriptomics analyses revealed overexpression of TaMGD enhances wheat plant heat stress resistance through multiple responses. *Ecotoxicol. Environ. Saf.* **290**, 117738 (2025).
23. Watson-Lazowski, A. et al. Multi-omic profiles of Sorghum genotypes with contrasting heat tolerance connect pathways related to thermotolerance. *J. Exp. Bot.* <https://doi.org/10.1093/jxb/erae506> (2024).
24. Das, A. et al. Metabolomic profiling of soybeans (*Glycine max* L.) reveals the importance of sugar and nitrogen metabolism under drought and heat stress. *Plants* **6**(2), 21 (2017).
25. Zhu, D. et al. Untargeted mass spectrometry-based metabolomics approach unveils molecular changes in heat-damaged and normal soybean. *Lwt* **171**, 114136 (2022).
26. Jha, U. C. et al. Metabolomic and lipidomic changes in heat-stressed chickpea seeds. *Front. Plant Sci.* **16**, 1668751. <https://doi.org/10.3389/fpls.2025.1668751> (2025).
27. Jha, U. C. et al. Heat stress-induced metabolomic shifts in chickpea (*Cicer arietinum* L.) flowers insights from contrasting genotypes. *Sci. Rep.* <https://doi.org/10.1038/s41598-025-21697-w> (2025).
28. Chianese, U. et al. Histone lysine demethylase inhibition reprograms prostate cancer metabolism and mechanics. *Mol. Metab.* **64**, 101561 (2022).
29. Wang, Y. et al. Cholestenoid acid as endogenous epigenetic regulator decreases hepatocyte lipid accumulation in vitro and in vivo. *Am. J. Physiol. Gastrointest. Liver Physiol.* **326**(2), G147–G162. <https://doi.org/10.1152/ajpgi.00184.2023> (2024).
30. Wold, S. et al. Principal component analysis. *Chemom. Intell. Lab. Syst.* **2**(1–3), 37–52 (1987).
31. Barker, M. & Rayens, W. Partial least squares for discrimination. *J. Chemom.* **17**(3), 166–173 (2003).
32. Eriksson L., et al. *Multi- and Megavariate Data Analysis, Part 1, Basic Principles and Applications: Umetrics AB.* (2006).
33. Kanehisa, M. & Goto, S. KEGG: Kyotoencyclopedia of genes and genomes. *Nucleic Acids Res.* **28**(1), 27–30. <https://doi.org/10.1093/nar/28.1.27> (2000).
34. Kanehisa, M. The KEGG databases at GenomeNet. *Nucleic Acids Res.* **30**(1), 42–46 (2002).
35. Nouri, Z. et al. On the neuroprotective effects of naringenin: Pharmacological targets, signaling pathways, molecular mechanisms, and clinical perspective. *Biomolecules* **9**(11), 690 (2019).
36. Daryanavard, H. et al. Flavonols modulate plant development, signaling, and stress responses. *Curr. Opin. Plant Biol.* **72**, 102350 (2023).
37. Jha, U. C. et al. Major abiotic stresses on quality parameters in grain legumes: Impacts and various strategies for improving quality traits. *Environ. Exp. Bot.* **228**, 105978 (2024).
38. Shahbaz, M. et al. Anticancer, antioxidant, ameliorative and therapeutic properties of kaempferol. *Int. J. Food Prop.* **26**, 1140–1166 (2023).
39. Laoué, J. et al. Plant flavonoids in mediterranean species: A focus on flavonols as protective metabolites under climate stress. *Plants* **11**, 172 (2022).
40. Duan, G. et al. Integrative transcriptomic and metabolomic analysis elucidates the vital pathways underlying the differences in salt stress responses between two chickpea (*Cicer arietinum* L.) varieties. *BMC Plant Biol.* **25**, 903 (2025).
41. Aarikan, B. et al. Protective role of quercetin and kaempferol against oxidative damage and photosynthesis inhibition in wheat chloroplasts under arsenic stress. *Physiol. Plant.* **175**(4), e13964 (2023).
42. Guan, Y. et al. Exploring heat stress responses and heat tolerance in rice in the reproductive stage: A dual omics approach. *Plant Growth Regul.* <https://doi.org/10.1007/s10725-025-01352-0> (2025).
43. Chen, Y. et al. Genes and pathways correlated with heat stress responses and heat tolerance in maize kernels. *Front. Plant Sci.* <https://doi.org/10.3389/fpls.2023.1228213> (2023).
44. Martinez, V. et al. Accumulation of flavonols over hydroxycinnamic acids favors oxidative damage protection under abiotic stress. *Front. Plant Sci.* **7**, 838 (2016).
45. Cui, J. et al. Flavonoids mitigate nanoplastic stress in *Ginkgo biloba*. *Plant Cell Environ* **48**(3), 1790–1811 (2025).
46. Ma, F. et al. Comprehensive analysis of bZIP transcription factors in passion fruit. *Iscience* <https://doi.org/10.1016/j.isci.2023.106556> (2023).
47. Mustafa, S. et al. Plant metabolite diosmin as the therapeutic agent in human diseases. *Curr. Res. Pharmacol. Drug Discov.* **3**, 100122 (2022).
48. Šamec, D. et al. The role of polyphenols in abiotic stress response: The influence of molecular structure. *Plants* **10**(1), 118 (2021).
49. Goleniowski, M. et al. Phenolic acids. In *Natural Products 1951–1973* (Springer, 2013).
50. Zhou, P. et al. Integrated analysis of transcriptomic and metabolomic data reveals critical metabolic pathways involved in polyphenol biosynthesis in *Nicotiana tabacum* under chilling stress. *Funct. Plant Biol.* **46**, 30–43 (2018).
51. Shu, P. et al. Ferulic acid enhances chilling tolerance in tomato fruit by up-regulating the gene expression of CBF transcriptional pathway in MAPK3-dependent manner. *Postharvest Biol. Technol.* **185**, 111775 (2022).
52. Karamzadeh, F. et al. Contribution of phenolic compounds and hormones in antioxidant defense responses of wild and cultivated barley genotypes under drought and heat stress. *Sci. Rep.* **15**, 27032 (2025).
53. Munir, K. et al. Ferulic acid mediated regulation of physiological and biochemical responses of maize (*Zea mays* L.) under heat stress. *J. Soil Sci. Plant Nutr.* **25**, 1–21 (2025).
54. Cheng, Z. Y. et al. Ferulic acid pretreatment alleviates heat stress in blueberry seedlings by inducing antioxidant enzymes, proline, and soluble sugars. *Biol. Plant.* **62**(3), 534–542 (2018).
55. Nagegowda, D. A. & Gupta, P. Advances in biosynthesis, regulation, and metabolic engineering of plant specialized terpenoids. *Plant Sci.* **294**, 110457 (2020).
56. Ninkuu, V. et al. Biochemistry of terpenes and recent advances in plant protection. *Int. J. Mol. Sci.* **22**(11), 5710 (2021).
57. Copolovici, L. et al. Emissions of green leaf volatiles and terpenoids from *Solanum lycopersicum* are quantitatively related to the severity of cold and heat shock treatments. *J. Plant Physiol.* **169**(7), 664–672 (2012).
58. Yesli, K. et al. Plant secondary metabolites produced in response to abiotic stresses has potential application in pharmaceutical product development. *Molecules* **27**(1), 313 (2022).

59. Shivashankar, K.S., et al. Association of volatile terpenoids and their biosynthetic genes in high temperature stress tolerance in tomato (*Solanum lycopersicum* L.). *J. Hort. Sci.* **19**(2), (2024).
60. Okereke, C. N. et al. Heat stress resistance drives coordination of emissions of suites of volatiles after severe heat stress and during recovery in five tropical crops. *Environ. Exp. Bot.* **184**, 104375 (2021).
61. Goswami, S. et al. Heat-responsive microRNAs regulate the transcription factors and heat shock proteins in modulating thermostability of starch biosynthesis enzymes in wheat (*Triticum aestivum* L.) under the heat stress. *Aust. J. Crop Sci.* **8**, 697–705 (2014).
62. Wilhelm, E. P. et al. Heat stress during grain filling in maize: Effects on kernel growth and metabolism. *Crop Sci.* **39**(6), 1733–1741 (1999).
63. Awasthi, R. et al. Individual and combined effects of transient drought and heat stress on carbon assimilation and seed filling in chickpea. *Funct. Plant Biol.* **41**(11), 1148–1167 (2014).
64. Yang, H. et al. Heat stress during grain filling affects activities of enzymes involved in grain protein and starch synthesis in waxy maize. *Sci. Rep.* **8**(1), 15665 (2018).
65. Serrano, N. et al. Thermopriming reprograms metabolic homeostasis to confer heat tolerance. *Sci. Rep.* **9**(1), 181 (2019).
66. Deng, Y. R. et al. Physicochemical properties and biological activity of broad bean protein hydrolysate obtained by membrane separation technology. *China Oils Fats* **47**, 92–99 (2022).
67. Ashihara, H. et al. Caffeine and related purine alkaloids: Biosynthesis, catabolism, function and genetic engineering. *Phytochemistry* **69**, 841–856 (2008).
68. Yoo, Y. et al. Caffeine produced in rice plants provides tolerance to water-deficit stress. *Antioxidants* **12**(11), 1984 (2023).
69. Miao, R. et al. The role of endogenous brassinosteroids in the mechanisms regulating plant reactions to various abiotic stresses. *Agron.* **14**(2), 356 (2024).
70. Luo, J. et al. Brassinosteroids promote thermotolerance through releasing BIN2-mediated phosphorylation and suppression of HsfA1 transcription factors in Arabidopsis. *Plant Commun.* **3**(6), 100419 (2022).
71. Kumari, A. & Hemantaranjan, A. Morpho-physiological attributes of wheat (*Triticum aestivum* L.) genotypes as influenced by brassinosteroids under heat stress. *J. Pharmacogn. Phytochem.* **7**(6), 2111–2115 (2018).
72. Lee, H. J. et al. Foliar application of biostimulants affects physiological responses and improves heat stress tolerance in Kimchi cabbage. *Hortic. Environ. Biotechnol.* **60**(6), 841–851 (2019).
73. Wang, W. et al. The exogenous application of brassinosteroids confers tolerance to heat stress by increasing antioxidant capacity in soybeans. *Agriculture* **12**(8), 1095 (2022).

Acknowledgements

UCJ thanks ICAR, New Delhi, for their support.

Generative AI statement

The author(s) declare that the latest version of Paperpal was used to check the grammar of this manuscript.

Author contributions

Uday C Jha: Formal analysis, Methodology, Validation, Visualization, Writing—original draft, Software. ****Shyam Tallury**** : Methodology, Writing—original draft, Writing—review & editing. ****Harsh Nayyar**** : Writing—review & editing. ****Kadambot H.M. Siddique**** Writing—interpretation of results, review & editing. ****Ignacio Ciampitti**** : Writing—interpretation of results, review & editing. ****P.V.**** Vara Prasad: Conceptualization, Supervision, Writing—original draft, Writing—review & editing.

Declarations

Competing interests

The authors declare no competing interests. Contribution Number 26-154-J from the Kansas Agricultural Experiment Station is acknowledged.

Additional information

Supplementary Information The online version contains supplementary material available at <https://doi.org/10.1038/s41598-026-40462-1>.

Correspondence and requests for materials should be addressed to U.C.J., H.N. or P.V.V.P.

Reprints and permissions information is available at www.nature.com/reprints.

Publisher's note Springer Nature remains neutral with regard to jurisdictional claims in published maps and institutional affiliations.

Open Access This article is licensed under a Creative Commons Attribution-NonCommercial-NoDerivatives 4.0 International License, which permits any non-commercial use, sharing, distribution and reproduction in any medium or format, as long as you give appropriate credit to the original author(s) and the source, provide a link to the Creative Commons licence, and indicate if you modified the licensed material. You do not have permission under this licence to share adapted material derived from this article or parts of it. The images or other third party material in this article are included in the article's Creative Commons licence, unless indicated otherwise in a credit line to the material. If material is not included in the article's Creative Commons licence and your intended use is not permitted by statutory regulation or exceeds the permitted use, you will need to obtain permission directly from the copyright holder. To view a copy of this licence, visit <http://creativecommons.org/licenses/by-nc-nd/4.0/>.

© The Author(s) 2026